SPATIO-TEMPORAL ANALYSIS OF BADLAND EXTENT IN SOUTHERN GUAM, MARIANA ISLANDS, USING TONAL ANALYSIS

Dr. Yuming Wen, Associate Professor of GIS
Maria Kottermair, Graduate Research Assistant
Dr. Mohammad Golabi, Associate Professor of Soil Science
Dr. Shahram Khosrowpanah, Professor of Water Resources Engineering
Water & Environmental Research Institute
University of Guam
Mangilao, GU 96923
ywen@uguam.uog.edu
mariakottermair@gmail.com
mgolabi@uguam.uog.edu
Khosrow@uguam.uog.edu

ABSTRACT

Soil erosion in the form of badlands is a common phenomenon throughout southern Guam. Badlands compared to any other land cover have the highest erosion rate. Consequently, they contribute the highest amount of sediments to the marine environment. Both human and natural factors may be responsible for badland development. To manage soil erosion, specifically on badlands, in an effective way, a better understanding of the processes associated with badland dynamics is essential. In this study we investigated how badland cover has changed between 1946 and 2006 in areas affected by human activities (off-roading and farming) and areas not affected by human activities. The badland cover classification was based on panchromatic and color aerial photography from 1946 and 1994, respectively; and QuickBird Satellite Imagery from 2006 using density slicing. A change detection analysis of the classified images from 1946, 1994, and 2006 identified areas of badland change. Preliminary results indicate that badland occurrence has increased during the aforementioned period. The badland in each study area changed in space and time. Future analyses will focus on natural factors like terrain attributes, soil characteristics, and high intensity rainstorms that influence badland dynamics.

Key Words: Quantitative spatial analysis; land cover change, geographic information system, badlands.

INTRODUCTION

Soil Erosion in southern Guam, Mariana Islands, creates fragmented landscapes in the form of large, orange-red colored patches of bare earth, so-called badlands. Soil erosion not only degrades the quality of the topsoil, but also severely impacts the water quality in streams and ocean, and ultimately impacts the health of Guam's coral reef system and marine flora and fauna. Badlands are one of the major contributors of soil erosion and associated sedimentation on Guam (Golabi *et al*., 2005; Scheman 2002). It is believed that natural factors such as terrain attributes (steep slopes) and natural events (*e.g.*, earthquakes, tropical cyclones, and high-intensity rainfall events) but also anthropogenic activities such as agriculture, arson grassfire, and off-roading affect badland development. To better understand the various factors influencing badland dynamics, especially the widely believed expansion of badlands, the actual change in badland cover in respect to land use needs to be studied first. In this study we are investigating the temporal and spatial patterns of badland occurrence over a 60-year period from 1946 to 2006 in areas with different land uses. We classified badlands based on historical aerial photos and satellite imagery using a geographic information system (GIS) to track changes in badland cover in three separate sites with different land uses.

STUDY AREA

The tropical island of Guam is the largest and southern-most island of the Mariana Archipelago in the Western North Pacific. It is located at 13° 28´ N and 144°45´ E. The elongated island has an area of 549 square kilometers.

The northern part of the island lies on a limestone plateau, while the southern part is primarily of volcanic origin with some limestone remnants along the ridges. The terrain in southern Guam is characterized by highly dissected uplands where badlands commonly occur.

We chose three separate subbasins with different land uses in central Southern Guam to quantify badland change and characterize relationship with land use. Typical badland sites were chosen for this study: Agat site (850 acres) located on the western side, and Talofofo site (860 acres) and Yona site (760 acres) on the eastern side of central Southern Guam. All three sites are undeveloped, except for some agricultural fields at the Talofofo site and few houses and streets along the boundary of the other two sites. The dominant land use is recreational, *e.g.*, hunting, hiking, and off-roading. The Agat site is considered no significant human impact on badlands, although hunters and hikers may use the area. The Yona site is a very popular off-roading area. The Talofofo site is primarily used for farming and off-roading; it is not clear whether the many tracks found in the area are from farm vehicles or recreational off-road vehicles (ORV).

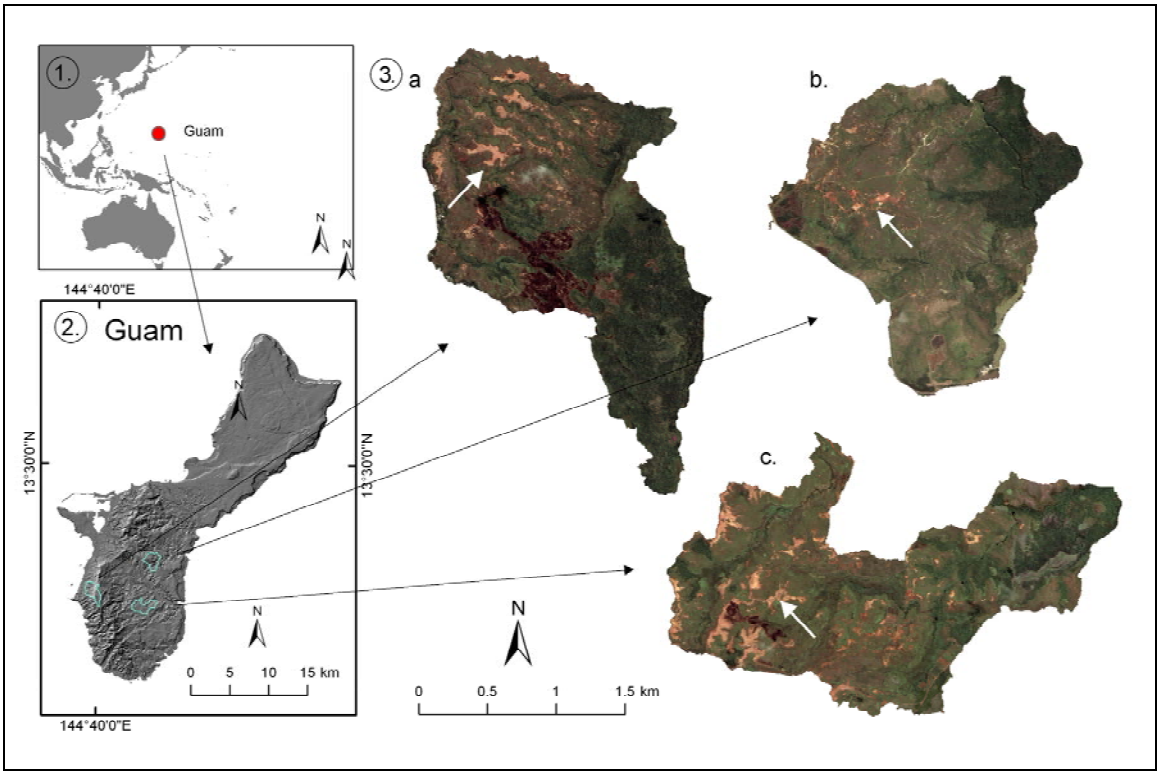

Figure 1. Maps of study area. (2) Regional map of the Western Pacific; (2) overview map of Guam with outline of study areas superimposed; (3) outline of study areas with 2006 QuickBird satellite imagery of a. Agat site, b. Yona site, and c. Talofofo site.

METHODS

Data Sources

The badland change detection analysis was based on two aerial photographs (1946 and 1994) and recent QuickBird satellite imagery (2006). Past badland extent was extracted from the oldest available panchromatic aerial photographs acquired in February 1946 and colored aerial photographs acquired in November 1994. The current badland extent was extracted from pan-sharpened 0.6-meter-resolution QuickBird Imagery taken between May 2005 and March 2006. One photograph per study site for 1946 and 1994 (a total of six) was selected based on the quality of the photograph (*e.g.*, cloud cover, resolution) and on location of the study area relative to the center of the photograph. Ideally, the area of interest should be as close to the center of the photograph as possible to reduce

distortion errors inflicted by the camera angle and topography. This, however, was not always achievable. To reduce the effect of fading towards the edge of the 1946 photographs, we adjusted contrast and brightness in Photoshop using a gradient mask. The scanned 1946 series we obtained had a resolution of 600 dpi. The 1994 series was a hard copy.

Data Processing

We scanned the 1994 series at a 1200 dpi resolution using an EPSON GT 10000 scanner. All further steps were performed in ArcGIS 9.3. We georectified each image based on the 2006 QuickBird imagery using a third-order polynomial transformation. A minimum of eleven ground control points (GCPs) with a total root mean square error (RMSE) of less than two meters for the 1946 and one meter for the 1994 series were selected in or along the boundary of each study area.

Classification and Analysis

We classified badlands based on grayscale values of the images. This method, called density slicing, categorizes an image based on user-defined grayscale/ brightness values (0-255) of a panchromatic photograph or a single band of a colored image. Mast et al. (1997) and Hudak and Wessmand (1998) applied density slicing in historical aerial photographs to determine tree cover and woody plants, respectively. This approach also seemed reasonable to discriminate badlands from the surrounding areas because badlands have generally a higher reflectance value in the visible light spectrum than other land cover types (mainly vegetation such as grassland and forest) found in the study areas. The high brightness values are especially pronounced in the red spectral band of the color images (1994 and 2006). The 1946 panchromatic photographs also show badlands in a higher gray value than surrounding land cover. Impervious surfaces (*e.g.*, roofs) and clouds also have a high reflectance value and could be considered as badlands by mistake using our approach; however, our study areas included only very few such surfaces and very few light cloud cover on few images which were manually removed after the density slicing was applied.

The range of grayscale values to classify badlands was determined for each image individually. The different types of input images (aerial and satellite images) and the variance in brightness and contrast even within a series required a unique threshold grayscale value for each image. The upper boundary of the brightness value for badlands was 255, the lower boundary was uniquely determined based on the input image. First, we identified the grayscale range that best represented current badland extent in all three study areas in the red band of the satellite imagery. One range (133-255) was selected for all three study areas since single satellite imagery covers the whole island and differences in illumination seemingly have been adjusted in the imagery processing. The satellite image was then reclassified into two categories (badland [*100*] and non-badland [*200*]) and resampled to one square meter. Next, we processed the remaining six rectified photographs from 1946 and 1994 accordingly. The badland 2006 raster from the first step was used as a guideline to determine the remaining grayscale values. To ensure classification consistency and not to over- or under-classify badlands in the different photographs, we based grayscale values on areas that appeared unchanged compared to the 2006 classification. Reclassification values for the 1994 photographs were *10* for badlands and *20* for non-badlands, and for the 1946 photographs *1* and *2*, respectively. All reclassified raster layers were clipped to the extent of the study areas. As aforementioned, impervious surfaces and clouds were manually removed or edited.

To detect changes in badland extent over time we performed an overlay analysis. All three reclassified raster layers for each study area were merged into one layer. The resulting pixel value represents the change this pixel experienced between 1946, 1994, and 2006. The value of each pixel (one square meter) from each reclassified raster layer (1946, 1994, and 2006) is either badland (BL) or not badland (NonBL). Here, we assigned values *1, 10, 100* to badlands for 1946, 1994, and 2006, respectively (*2, 20, and 200* to not badland, respectively). All three raster layers were added in the raster calculator, resulting in a new raster layer. Each pixel is assigned a new value which is the sum of the values of three input pixels; *e.g*, for NonBL-BL-BL (1946-1994-2006), the result would be 112 (2+10+100). The change detection logic is presented in Figure 2.

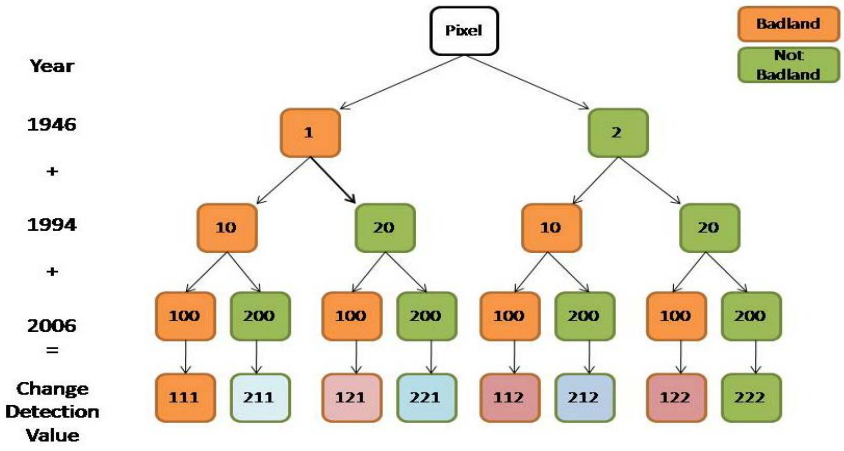

Figure 2. Badland Change Detection Logic of all input values and outcome values from the pixel analysis.

RESULTS AND DISCUSSION

Image processing of aerial photographs and satellite imagery quantified areas covered by badlands in 1946, 1994, and 2006 (Table 1). Overall, badland cover increased at all three sites during the 60-year study period. In the Agat site, badlands increased from 3.5% (30 acres) of the total area in 1946 to 4.0% (35 acres) in 2006. In the Yona site, badlands increased from 2.8% (21.5 acres) of the total area to 4.4% (33.5 acres) in the same time period. In the Talofofo site, badlands increased from 7% (60.3 acres) in 1946 to 9.7% (81.8 acres) in 1994, but then decreased to 8.0% (68.3 acres) in 2006. The greatest increase in badland cover at any period (1946-1994 and 1994-2006) occurred in the Yona site between 1946 and 1994 where the area of badlands was more than doubled (51%) during that time. The total badland cover of all three sites increased by 31.8% between 1946 and 1994, but then decreased by 7.2% between 1994 and 2006. However, considering the 60-year period the total badland cover still increased by 22.3%. In addition, slight increase of badland areas for Agat and Yona subbasins and decrease of badland area in the Talofofo site from 1994 to 2006 resulted in the total decrease in badland cover for such a period. See Table 1 for details. Figure 3 shows the badland change in the study areas from 1946 to 2006, and the meanings of different codes can be obtained from Figure 2. More details about badland dynamics between different years and sites are listed in Table 2. Research about impacts of more factors on badland dynamics will be conducted in the near future.

Table 1. Statistical breakdown of the area (acres/ percent of study site) covered by badlands in 1946, 1994, and 2006 and the change (%) between these years at three study sites.

	Badland Cover						Total Area	Change of Badland Cover		
	1946		1994		2006			1946-1994	1994-2006	1946-2006
	acres	%	acres	%	acres	%	acres	%	%	%
Agat	30.0	3.5	33.0	3.8	35.0	4.0	869.6	10.0	6.0	16.6
Talofofo	60.3	7.0	81.8	9.7	68.3	8.0	856.8	35.7	-16.5	13.2
Yona	21.5	2.8	32.5	4.3	33.5	4.4	757.7	51.2	3.0	55.8
Total	111.8	4.5	147.4	5.9	136.8	5.5	2484.1	31.8	-7.2	22.3

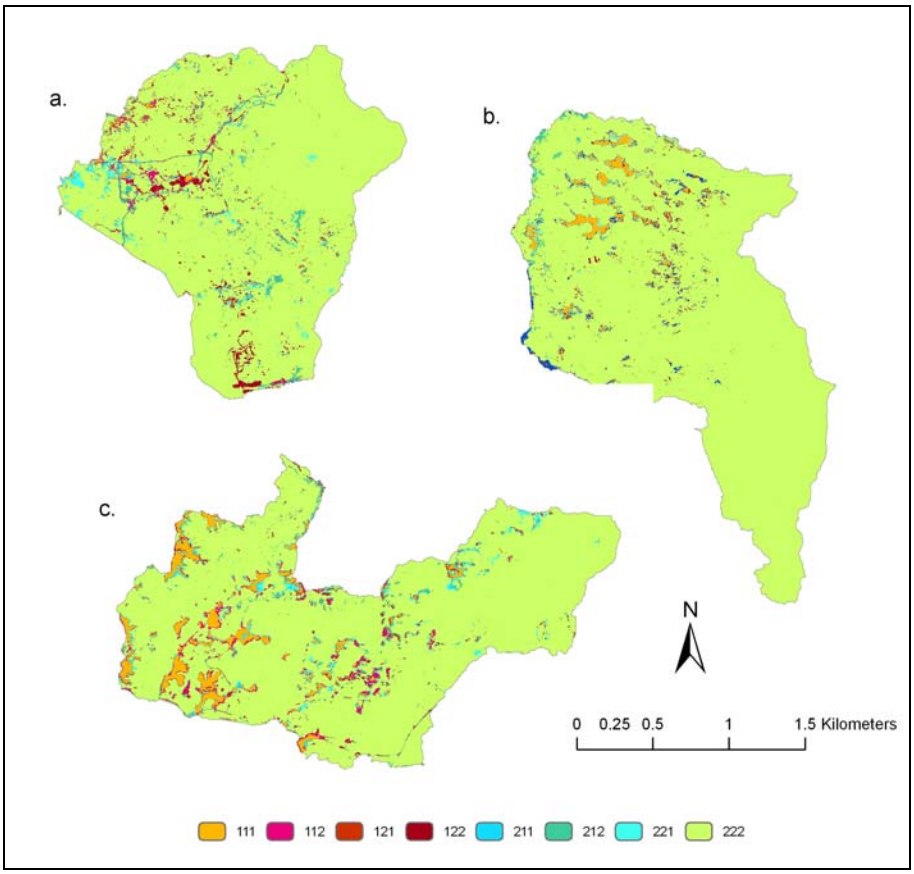

Figure 3. Badland change detection maps of the three study sites from 1946 to 1994 to 2006. Areas where no change occurred during the study period have a value of 111 for badland and 222 for not badland, respectively. All other areas experience some kind of change. (a) Yona site, (b) Agat site, and (c) Talofofo site. Code legend is explained in Figure 2.

Table 2. Result of badland change (acres/ percent) at three sites from 1946 to 1994 and to 2006. Code legend is explained in Figure 2.

	Area of Badland Cover					
	acres			%		
Code	Agat	Yona	Talofofo	Agat	Yona	Talofofo
111	16.78	3.28	37.72	1.93	0.43	4.40
112	6.77	8.60	16.14	0.78	1.13	1.88
121	1.88	1.74	3.76	0.22	0.23	0.44
122	9.59	19.89	10.67	1.10	2.62	1.25
211	2.26	2.46	6.23	0.26	0.32	0.73
212	7.21	18.17	21.74	0.83	2.40	2.54
221	9.12	14.02	12.60	1.05	1.85	1.47
222	816.03	689.55	747.89	93.84	91.00	87.29
Total	869.63	757.71	856.75	100.00	100.00	100.00

ACKNOWLEDGEMENTS

This research was funded partly by an Environmental Science Scholarship funded by National Oceanic and Atmospheric Administration (NOAA) Office of Ocean and Coastal Resources Management through the University of Guam Water and Environmental Research Institute (WERI) via Guam Bureau of Statistics and Plans, Guam Coastal Management Program (GCMP) (Award#: NA07NOS4190177), and partly by U.S. Geological Survey (USGS) Water Resources Research Institute 104B Program (Award#: 02HQGR0134) and Guam Hydrological Survey.

REFERENCES

Golabi, M.H., C. Iyekar, D. Minton, C.L. Raulerson, and D. Chargualaf, 2005. Watershed management to meet water quality standards by using the Vetiver System in Southern Guam, *AU J.I.*, 9(1): 64–70.

Hudak, A.T, and C.A. Wessman, 1998. Textural analysis of historical aerial photography to characterize woody plant encroachment in South African Savanna, *Remote Sensing Environment*, 66:317-330.

Mast, J.N., T.T. Veblen, and M.E. Hodgson, 1997. Tree Invasion within a pine/grassland ecotone: An approach with historic aerial photographs and GIS modeling, *Forest Ecology and Management*, 93:181-194.

Scheman, N., 2002. Identification of Erosion Processes and Sources of Exposed Patches in the La Sa Fua Watershed of Southern Guam, M.S. Thesis, Water and Environmental Research Institute, University of Guam.